

# COMPREHENSIVE KINEMATICS AND KINETICS OF COSSERAT BEAMS AND THEIR APPLICATION FOR DEVELOPING A MEASUREMENT MODEL FOR STRAIN GAUGES

MAYANK CHADHA<sup>1</sup> AND MICHAEL D. TODD<sup>2</sup>

<sup>1</sup> University of California, San Diego  
9500 Gilman Drive, La Jolla CA 92092-0085  
machadha@eng.ucsd.edu

<sup>2</sup> University of California, San Diego  
9500 Gilman Drive, La Jolla CA 92092-0085  
mdtodd@ucsd.edu

**Key words:** Cosserat beam, Coupled Poisson's and warping effect, Cross-sectional deformation, strain gauges, finite strain and large deformations

**Abstract.** Our research on reconstructing the global deformed shape of the rod-like structure using measurements from a finite number of surface strain gauge, has led us to investigate and improve the kinematics of Cosserat beams subjected to large deformation and finite strain. In this work, we present an exhaustive, geometrically exact, non-linear kinematics model that captures deformation due to multiple curvatures, torsion, shear, axial deformation, warping and fully-coupled Poisson's effect. We develop the deformation gradient tensor and detail the contribution of various deformation effects. The kinematics developed here is used to establish a measurement model of discrete and finite length strain gauge attached to the surface of the beam or embedded into the beam. We briefly discuss the expression for the internal power of such a beam.

## 1 INTRODUCTION

Strain gauges are devices of significant importance used for wide variety of measurement and structural health monitoring applications including but not limited to civil structures, biomedical systems, and aerospace structures. Many of these monitoring applications involve single manifold characterized structures such as pipelines, suspension cables, tethers, surgical tubings, etc. These kind of structures may be modeled by framed space curves as suggested by Duhem [1] and the Cosserat brothers [2]. It is therefore, desirable to develop a refined and complete kinematics of Cosserat rods with the aim of developing a measurement model for finite length or discrete strain gauges attached on to the surface or embedded into these rods.

Most of the work on Cosserat rod theory including that of Eric Reissner [3]-[5], Simo [6], Simo and Vu-Quoc [7], Kapania and Li [8] and Meier [9] focused more on the numerical

solutions of the governing equations of motion and less on cross-sectional deformation. This is well justified because the slender nature of the structure prompts the Euler-Bernoulli rigid cross-section assumption. However, in the field of shape sensing (and structural health monitoring), the cross-sectional deformation is crucial. The work of Simo and Vu-Quoc does consider warping of unsymmetrical cross-section by using the concept of shear center. The approach introduces *warping amplitude* as an additional finite strain parameter and is well suited for finite element solution for such problem.

In this paper, we present a comprehensive kinematic model of Cosserat rods such that cross-sectional deformations are permitted and further develop a measurement model for the strain gauges. We briefly discuss the expression of the stress power considering the kinematics developed in this work. The results presented here are in fact part of developing a general shape sensing methodology as an extension of the authors previous work Todd et al. [10] and Chadha and Todd [11]-[13].

The remainder of the paper is arranged as follows: section 2 discusses various mathematical tools and the geometry of the undeformed and deformed states. Section 3 presents the expression of the strain vector and deformation gradient tensor of the beam. Section 4 derives the expression of the scalar strains of the finite length and the discrete strain gauges. In section 5 we discuss the stress power for such kinematics. Section 6 concludes the paper.

## 2 MATHEMATICAL TOOLS AND GEOMETRY OF VARIOUS CONFIGURATIONS

The reference beam configuration can be initially curved or straight. Prior knowledge of the initially curved reference configuration allows us to define a map from the curved reference configuration to a mathematically straight reference configuration  $\Omega_0$  (refer Chadha and Todd [14]). In this paper, we shall consider the undeformed beam configuration to be  $\Omega_0$ . The final deformed configuration  $\Omega_3$  that incorporates warping and complete Poisson's effect is defined with respect to an intermediate beam configuration  $\Omega_1$  that employs the Euler-Bernoulli rigid cross section assumption.

Consider a fixed orthogonal triad  $\{\mathbf{E}_i\}$ . Any point in the undeformed configuration  $\Omega_0$  is defined by the position vector  $\mathbf{R}_0 = \xi_i \mathbf{E}_i$ . The family of cross-section constituting the configuration  $\Omega_0$  is represented by  $\blacksquare_0(\xi_1)$ . The material coordinates  $(\xi_1, \xi_2, \xi_3)$ , represents any point in the beam irrespective of the deformed configuration. The configuration of  $\Omega_1$  is defined by a framed space curve (called as midcurve)  $\boldsymbol{\varphi}(\xi_1) = \varphi_i \mathbf{E}_i \in \mathbb{R}^3$  and the family of cross-sections  $\blacksquare_1(\xi_1) = \{(\xi_2, \xi_3) \in \mathbb{R}_{\xi_1}^2\}$ , parametrized by the undeformed arc-length  $\xi_1 \in [0, L_0]$ . Here,  $\mathbb{R}_{\xi_1}^2$  represents a 2D Euclidean space spanned by the orthonormal directors  $\mathbf{d}_2(\xi_1) - \mathbf{d}_3(\xi_1)$  and the director  $\mathbf{d}_1(\xi_1)$  is normal to  $\mathbb{R}_{\xi_1}^2$  such that the orthonormal triad  $\{\mathbf{d}_i(\xi_1)\}$  with its origin at  $\boldsymbol{\varphi}(\xi_1)$  represents the director triad spanning the 3D Euclidean space  $\mathbb{R}_{\xi_1}^3$ . The midcurve can be defined as locus of family of cross-sections or the locus of the shear center (as in Simo and Vu-Quoc [7]). Essentially it is a reference curve with respect to which, a point on the cross-section can be located. We define the

map  $\mathbf{R}_1 : \Omega_0 \longrightarrow \Omega_1$  such that,

$$\mathbf{R}_1 = \boldsymbol{\varphi}(\xi_1) + \xi_2 \mathbf{d}_2(\xi_1) + \xi_3 \mathbf{d}_3(\xi_1). \quad (1)$$

The triad  $\{\mathbf{E}_i\}$  and  $\{\mathbf{d}_i\}$  are related to each other by means of proper orthogonal tensor  $\mathbf{Q} \in SO(3)$  such that,

$$\begin{aligned} \mathbf{d}_i &= \mathbf{Q} \mathbf{E}_i; \\ \mathbf{Q} &= \mathbf{d}_i \otimes \mathbf{E}_i. \end{aligned} \quad (2)$$

The evolution of the framed space curve is governed by the derivatives of the midcurve position vector  $\boldsymbol{\varphi}_{,\xi_1}$  and the derivative of the director triad  $\{\mathbf{d}_{i,\xi_1}\}$ . We define the deformed arc-length as  $s(\xi_1)$ , such that  $\boldsymbol{\varphi}_{,s}$  represents the tangent vector to the midcurve such that,

$$\begin{aligned} \boldsymbol{\varphi}_{,\xi_1} &= (1+e)\boldsymbol{\varphi}_{,s} = (1+e)(\cos \gamma_{11} \mathbf{d}_1 + \sin \gamma_{12} \mathbf{d}_2 + \sin \gamma_{13} \mathbf{d}_3); \\ e(\xi_1) &= \frac{ds}{d\xi_1} - 1 := \text{axial strain}. \end{aligned} \quad (3)$$

Here,  $\gamma_{1i}(\xi_1)$ , for  $i = 1 \dots 3$  represents the shear angles. From Eq. (2), we have,

$$\mathbf{d}_{i,\xi_1} = \mathbf{Q}_{,\xi_1} \mathbf{Q}^T \mathbf{d}_i = \mathbf{K} \mathbf{d}_i = \boldsymbol{\kappa} \times \mathbf{d}_i. \quad (4)$$

Note that  $\mathbf{Q}_{,\xi_1} \in T_{\mathbf{Q}}SO(3)$  where,  $T_{\mathbf{Q}}SO(3)$  represents the tangent space to  $SO(3)$  at some  $\mathbf{Q} \in SO(3)$ . Secondly,  $\mathbf{Q}_{,\xi_1} \mathbf{Q}^T = \mathbf{K}(\xi_1)$  is skew-symmetric matrix that has Darboux vector  $\boldsymbol{\kappa}(\xi_1) = \bar{\kappa}_i \mathbf{d}_i$  as the corresponding axial vector.

Finally, we define another configuration  $\Omega_2$  that incorporates warping in the same sense of Simo and Vu-Quoc [7] such that the mapping  $\mathbf{R}_2 : \Omega_0 \longrightarrow \Omega_2$  is defined as

$$\mathbf{R}_2 = \boldsymbol{\varphi}(\xi_1) + \xi_2 \mathbf{d}_2(\xi_1) + \xi_3 \mathbf{d}_3(\xi_1) + p(\xi_1) \Psi(\xi_2, \xi_3) \mathbf{d}_1 = \mathbf{R}_1 + p(\xi_1) \Psi(\xi_2, \xi_3) \mathbf{d}_1, \quad (5)$$

where  $p$  represents the warping amplitude. We need this intermediate configuration to develop a comprehensive kinematic model that will define the final deformed configuration  $\Omega_3$  of the beam.

### 3 KINEMATICS OF VARIOUS DEFORMED STATES

We use the index  $j$  to represent any quantity associated with the deformed state  $\Omega_j$  with  $j = 1, 2, 3$ .

#### 3.1 Deformation gradient tensor and the strain vectors for the configuration $\Omega_j$

Let  $p = (\xi_1, \xi_2, \xi_3) \in \Omega_0$ . We define the two point deformation gradient tensor as a differential map  $\mathbf{F}_j : T_p \Omega_0 \longrightarrow T_{\mathbf{R}_j(p)} \Omega_j$  such that,

$$\mathbf{F}_j = \frac{d\mathbf{R}_j}{d\mathbf{R}_0} = \mathbf{R}_{j,\xi_i} \otimes \mathbf{E}_i. \quad (6)$$

Consider the special case with  $j = 1$ , the first component of infinitesimal vector  $d\mathbf{R}_0$  strains, whereas the other two components just experience rotation because of Euler-Bernoulli's rigid cross-section assumption in the configuration  $\Omega_1$  (refer section 3.1.1 of Chadha and Todd [14]). However, the second and third component of any vector experiences strain when we incorporate Poisson's and warping effect (for  $j = 2 - 3$ ) as we will see shortly. We define three ( $i = 1, 2, 3$ ) strain vectors  $\boldsymbol{\lambda}_i^j = \bar{\lambda}_{ik}^j \mathbf{d}_k$  such that,

$$\boldsymbol{\lambda}_i^j = \mathbf{R}_{j,\xi_i} - \mathbf{d}_i = \mathbf{F}_j \mathbf{E}_i - \mathbf{d}_i. \quad (7)$$

Therefore, from Eq. (6) and (7), we have,

$$\mathbf{F}_j = \boldsymbol{\lambda}_i^j \otimes \mathbf{E}_i + \mathbf{Q}. \quad (8)$$

In the component form,

$$[\mathbf{F}_j]_{\mathbf{d}_p \otimes \mathbf{E}_q} = [\bar{\mathbf{F}}_j]_{\mathbf{E}_p \otimes \mathbf{E}_q} = \overbrace{\begin{bmatrix} \langle \boldsymbol{\lambda}_1^j, \mathbf{d}_1 \rangle & \langle \boldsymbol{\lambda}_2^j, \mathbf{d}_1 \rangle & \langle \boldsymbol{\lambda}_3^j, \mathbf{d}_1 \rangle \\ \langle \boldsymbol{\lambda}_1^j, \mathbf{d}_2 \rangle & \langle \boldsymbol{\lambda}_2^j, \mathbf{d}_2 \rangle & \langle \boldsymbol{\lambda}_3^j, \mathbf{d}_2 \rangle \\ \langle \boldsymbol{\lambda}_1^j, \mathbf{d}_3 \rangle & \langle \boldsymbol{\lambda}_2^j, \mathbf{d}_3 \rangle & \langle \boldsymbol{\lambda}_3^j, \mathbf{d}_3 \rangle \end{bmatrix}}^{\text{displacement gradient tensor } [\nabla_{\Omega_0} \mathbf{u}_j]_{\mathbf{d}_p \otimes \mathbf{E}_q}} + \overbrace{\begin{bmatrix} 1 & 0 & 0 \\ 0 & 1 & 0 \\ 0 & 0 & 1 \end{bmatrix}}^{\mathbf{I}_3}; \quad (9)$$

$$[F_{j_{pq}}]_{\mathbf{d}_p \otimes \mathbf{E}_q} = \langle \boldsymbol{\lambda}_q^j, \mathbf{d}_p \rangle + \delta_{pq}.$$

Here,  $\langle \cdot, \cdot \rangle$  represents the inner product. The displacement field for the deformed configuration is given by  $\mathbf{u}_j = \mathbf{R}_j - \mathbf{R}_0$ . We define *material form* of the deformation gradient tensor and the strain vector respectively as

$$\begin{aligned} \bar{\mathbf{F}}_j &= \mathbf{Q}^T \mathbf{F}_j \mathbf{I}_3 = \bar{\boldsymbol{\lambda}}_i^j \otimes \mathbf{E}_i + \mathbf{I}_3; \\ \bar{\boldsymbol{\lambda}}_i^j &= \mathbf{Q}^T \boldsymbol{\lambda}_i^j. \end{aligned} \quad (10)$$

We define the midcurve strain vector as  $\boldsymbol{\varepsilon} = \bar{\varepsilon}_i \mathbf{d}_i$  such that

$$\boldsymbol{\varepsilon} = \boldsymbol{\varphi}_{,\xi_1} - \mathbf{d}_1 = ((1 + e) \cos \gamma_{11} - 1) \mathbf{d}_1 + ((1 + e) \sin \gamma_{12}) \mathbf{d}_2 + ((1 + e) \sin \gamma_{13}) \mathbf{d}_3 \quad (11)$$

From the definition of the material deformation gradient tensor, we can obtain the time derivative of  $\mathbf{F}_j$  as

$$\begin{aligned} \dot{\mathbf{F}}_j &= \dot{\mathbf{Q}} \mathbf{Q}^T \mathbf{F}_j + \dot{\bar{\mathbf{F}}}_j; \\ \dot{\bar{\mathbf{F}}}_j &= \mathbf{Q}^T \dot{\bar{\mathbf{F}}}_j \mathbf{I}_3 = \dot{\bar{\boldsymbol{\lambda}}}_i^j \otimes \mathbf{E}_i; \\ \dot{\bar{\mathbf{F}}}_j &= \dot{\bar{\boldsymbol{\lambda}}}_i^j \otimes \mathbf{E}_i \end{aligned} \quad (12)$$

In the equation above,  $\dot{\bar{\mathbf{F}}}$  and  $\dot{\bar{\boldsymbol{\lambda}}}_i^j$  is defined as the co-rotated time derivative of the deformation gradient tensor and the strain vector respectively (refer section 2.2.4. of Chadha and Todd [14]). These quantities are useful to define the stress power of the beam.

### 3.2 Coupled Poisson's transformation and the final deformed state

To define a coupled Poisson's effect, we first obtain the strain vectors for the configuration  $\Omega_2$ . These can be obtained using the equations (3), (5), (7) and (11) as

$$\begin{aligned}\boldsymbol{\lambda}_1^2 &= (\bar{\varepsilon}_1 + \xi_3 \bar{\kappa}_2 - \xi_2 \bar{\kappa}_3 + (p\Psi)_{,\xi_1}) \mathbf{d}_1 + (\bar{\varepsilon}_2 - \xi_3 \bar{\kappa}_1 + p\Psi \bar{\kappa}_3) \mathbf{d}_2 \\ &\quad + (\bar{\varepsilon}_3 + \xi_2 \bar{\kappa}_1 - p\Psi \bar{\kappa}_2) \mathbf{d}_3; \\ \boldsymbol{\lambda}_i^2 &= (p\Psi)_{,\xi_i} \mathbf{d}_1 \text{ for } i = 2, 3.\end{aligned}\tag{13}$$

It is clear from the above expression that the axial strain along the director  $\mathbf{d}_1$  is given by  $\langle \boldsymbol{\lambda}_1^2, \mathbf{d}_1 \rangle = [\nabla_{\Omega_0} \mathbf{u}_2]_{\mathbf{d}_1 \otimes \mathbf{E}_1} = [\mathbf{F}_2]_{\mathbf{d}_1 \otimes \mathbf{E}_1} - 1$ . Therefore, we define the coupled Poisson's transformation as

$$\hat{\xi}_i = (1 - \nu(\xi_1, \xi_2, \xi_3) \langle \boldsymbol{\lambda}_1^2, \mathbf{d}_1 \rangle) \xi_i \text{ for } i = 2 - 3.\tag{14}$$

Note that there are primarily 7 unknown section strain parameters  $(\bar{\varepsilon}_1, \bar{\varepsilon}_2, \bar{\varepsilon}_3, \bar{\kappa}_1, \bar{\kappa}_2, \bar{\kappa}_3, p)$  and inclusion of Poisson's effect does not add any new strain parameter. Secondly, for generality, we assume inhomogeneous material implying that the Poisson's ratio field  $\nu(\xi_1, \xi_2, \xi_3)$  is not a constant.

We can now define the map  $\mathbf{R}_3 : \Omega_0 \rightarrow \Omega_3$  such that

$$\mathbf{R}_3 = \boldsymbol{\varphi}(\xi_1) + \hat{\xi}_2 \mathbf{d}_2(\xi_1) + \hat{\xi}_3 \mathbf{d}_3(\xi_1) + p(\xi_1) \Psi(\xi_2, \xi_3) \mathbf{d}_1.\tag{15}$$

The family of cross-sections  $\blacksquare_2(\xi_1) = \{(\xi_2, \xi_3, p\Psi) \in \mathbb{R}_{\xi_1}^3\}$  and  $\blacksquare_3(\xi_1) = \{(\hat{\xi}_2, \hat{\xi}_3, p\Psi) \in \mathbb{R}_{\xi_1}^3\}$  associated with the deformed configurations  $\Omega_2$  and  $\Omega_3$  respectively, are no longer planar. The strain vectors for the configuration  $\Omega_3$  are obtained as

$$\begin{aligned}\boldsymbol{\lambda}_1^3 &= \left( \bar{\varepsilon}_1 + \hat{\xi}_3 \bar{\kappa}_2 - \hat{\xi}_2 \bar{\kappa}_3 + (p\Psi)_{,\xi_1} \right) \mathbf{d}_1 + \left( \bar{\varepsilon}_2 - \hat{\xi}_3 \bar{\kappa}_1 + \hat{\xi}_2 \bar{\kappa}_1 + p\Psi \bar{\kappa}_3 \right) \mathbf{d}_2 \\ &\quad + \left( \bar{\varepsilon}_3 + \hat{\xi}_2 \bar{\kappa}_1 + \hat{\xi}_3 \bar{\kappa}_1 - p\Psi \bar{\kappa}_2 \right) \mathbf{d}_3; \\ \boldsymbol{\lambda}_2^3 &= \left( \hat{\xi}_2 \bar{\kappa}_2 - 1 \right) \mathbf{d}_2 + \hat{\xi}_3 \bar{\kappa}_2 \mathbf{d}_3 + (p\Psi)_{,\xi_2} \mathbf{d}_1; \\ \boldsymbol{\lambda}_3^3 &= \left( \hat{\xi}_3 \bar{\kappa}_3 - 1 \right) \mathbf{d}_3 + \hat{\xi}_2 \bar{\kappa}_3 \mathbf{d}_2 + (p\Psi)_{,\xi_3} \mathbf{d}_1.\end{aligned}\tag{16}$$

Unlike  $\mathbf{F}_1$  and  $\mathbf{F}_2$ , the components of the deformation gradient tensor  $\mathbf{F}_3$  forms a fully populated matrix as seen from Eq.(9).

### 3.3 Physical interpretation of the strain vectors $\boldsymbol{\lambda}_i^j$

Consider a point  $p \in \Omega_0$ . The vector  $\boldsymbol{\lambda}_i^j$  represents the strain vector at a point  $\mathbf{R}_3(p) \in \Omega_j$  corresponding to the vector  $\mathbf{E}_i \in T_p \Omega_0$ . The vector  $d\mathbf{R}_0 = d\xi_i \mathbf{E}_i \in T_p \Omega_0$  gets strained (the contribution due to  $\boldsymbol{\lambda}_i^j \otimes \mathbf{E}_i$  in  $\mathbf{F}_j$ ) and undergoes rigid body rotation (the contribution due to  $\mathbf{Q}$ ). The tensor product  $\boldsymbol{\lambda}_i^j \otimes \mathbf{E}_i$  filters out the  $i^{\text{th}}$  component of the vector  $d\mathbf{R}_0 = d\xi_i \mathbf{E}_i$  and strains it along the vector  $\boldsymbol{\lambda}_i^j$ . Figure 1 shows the deformation of the unit vector  $\mathbf{E}_1 \in T_p \Omega_0$ , deformed to the vector  $\mathbf{F}_3 \mathbf{E}_1 = \boldsymbol{\lambda}_1^3 + \mathbf{d}_1$ . Each subsequent step in the flowchart does not represent superimposition, but is mere inclusion of different deformation effects at each progressive step.

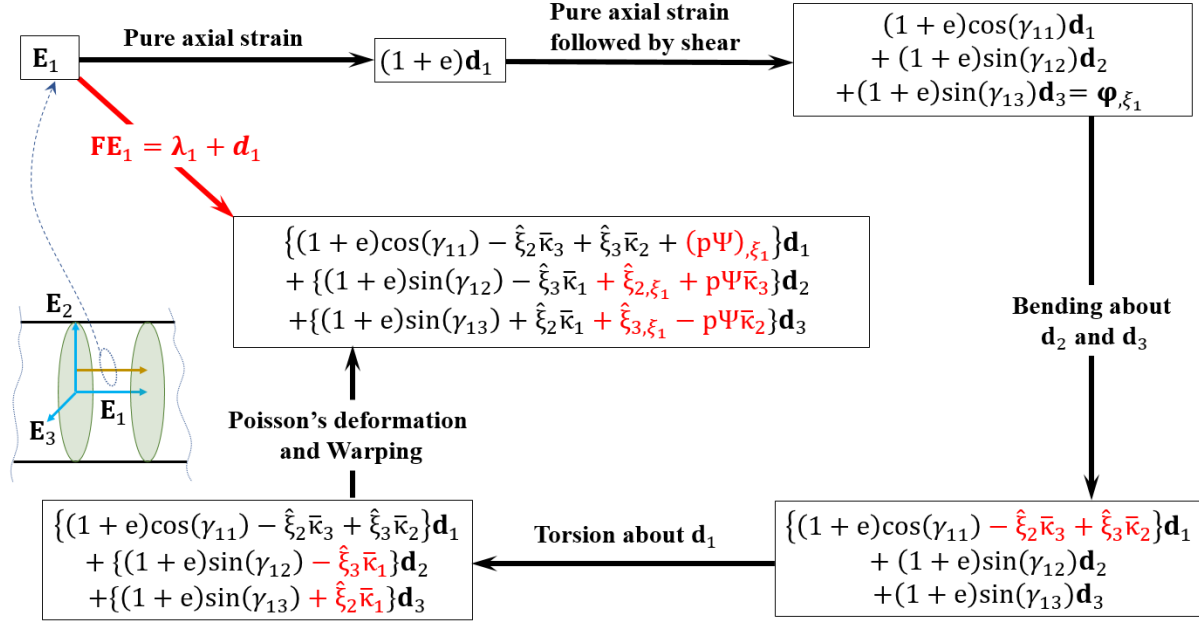


**Figure 1:** Flowchart showing deformation of the unit vector  $\mathbf{E}_1 \in T_p\Omega_0$  considering final deformed configuration is  $\Omega_3$ .

## 4 MEASUREMENT MODEL FOR DISCRETE AND FINITE LENGTH STRAIN GAUGE

### 4.1 Finite length strain gauge

Consider the deformed state to be  $\Omega_3$ . We can model a finite length strain gauge as a curve. Consider the unstrained segment of FBG sensor as a space curve  $\boldsymbol{\alpha} : [0, l_0] \rightarrow \Omega_0$  such that  $\boldsymbol{\alpha}(t) = \xi_i(t)\mathbf{E}_i$  where the parameter  $t \in [0, l_0]$ . The curve  $\boldsymbol{\alpha}(t)$  maps to the curve  $\boldsymbol{\beta}(t) = \mathbf{R}_3(\boldsymbol{\alpha}(t)) : [0, l_0] \rightarrow \Omega_3$ , such that for the vector  $\boldsymbol{\alpha}_{,t}(t) \in T_{\boldsymbol{\alpha}(t)}\Omega_0$ , we have  $\boldsymbol{\beta}_{,t}(t) = \mathbf{F}_3\boldsymbol{\alpha}_{,t}(t) : [0, l_0] \rightarrow T_{\boldsymbol{\beta}(t)}\Omega_3$ . The magnitude of the tangent vector  $\boldsymbol{\beta}_{,t}(t)$  can be obtained as

$$|\boldsymbol{\beta}_{,t}(t)| = \langle \boldsymbol{\beta}_{,t}(t), \boldsymbol{\beta}_{,t}(t) \rangle^{\frac{1}{2}} = \langle \mathbf{F}_3\boldsymbol{\alpha}_{,t}(t), \mathbf{F}_3\boldsymbol{\alpha}_{,t}(t) \rangle^{\frac{1}{2}} = \sqrt{C_{3pq}\alpha_{p,t}\alpha_{q,t}}. \quad (17)$$

Here,  $\mathbf{C}_3 = \mathbf{F}_3^T \mathbf{F}_3$  represents the *right Cauchy Green deformation tensor* which can be thought as a *Push-forward Riemann metric* in the deformed configuration  $\Omega_3$ . The length of the curve  $\boldsymbol{\beta}(t)$  is obtained as

$$l(t) = \int_0^t |\boldsymbol{\beta}_{,t}(k)| dk = \int_0^t \sqrt{[C_{3pq}\alpha_{p,t}\alpha_{q,t}]_{(t=k)}} dk, \quad (18)$$

and the average scalar strain value at the material point  $(\xi_1(t), \xi_2(t), \xi_3(t)) \in \Omega_3$  is

$$\varepsilon_{\text{finite}}(t) = \frac{l(t)}{t} - 1. \quad (19)$$

## 4.2 Discrete strain gauge

A discrete strain gauge can be treated as a small vector  $l_g \mathbf{n} \in T_p \Omega_0$  such that its orientation  $\mathbf{n}$  (unit vector) and the gauge length  $l_g$  in the undeformed state  $\Omega_0$  is known. Here,  $p = (\xi_1^g, \xi_2^g, \xi_3^g) \in \Omega_0$  represents the point of attachment of the strain gauge.

The vector  $\mathbf{r}^g = \xi_2^g \mathbf{E}_2 + \xi_3^g \mathbf{E}_3$  locates the point  $p$  with respect to the midcurve on the cross-section  $\blacksquare_0$ . The tangent plane  $T_p \Omega_0$  can be identified with  $\mathbb{R}^2$  if the strain gauge is attached to the surface of the beam, or else it can be identified with  $\mathbb{R}^3$  if the strain gauge is embedded in the beam. Let us assume that the strain gauge is attached to the surface of the beam. The tangent plane  $T_p \Omega_0$  is then spanned by the unit orthonormal vectors  $\mathbf{t} - \tilde{\mathbf{t}}$  such that

$$\tilde{\mathbf{t}} = \cos \tilde{\mu} \mathbf{E}_1 + \sin \tilde{\mu} \left( \frac{\mathbf{r}^g}{|\mathbf{r}^g|} \right) = \cos \tilde{\mu} \mathbf{E}_1 + \left( \frac{\xi_2^g \sin \tilde{\mu}}{\sqrt{\xi_2^{g2} + \xi_3^{g2}}} \right) \mathbf{E}_2 + \left( \frac{\xi_3^g \sin \tilde{\mu}}{\sqrt{\xi_2^{g2} + \xi_3^{g2}}} \right) \mathbf{E}_3. \quad (20)$$

The vector  $\mathbf{t}$  represents the unit tangent vector to the periphery  $\Gamma_0$  of the cross-section  $\blacksquare_0$  ( $\xi_1^g$ ), such that

$$\mathbf{t} = \mathbf{E}_1 \times \left( \frac{\mathbf{r}^g}{|\mathbf{r}^g|} \right) = - \left( \frac{\xi_3^g}{\sqrt{\xi_2^{g2} + \xi_3^{g2}}} \right) \mathbf{E}_2 + \left( \frac{\xi_2^g}{\sqrt{\xi_2^{g2} + \xi_3^{g2}}} \right) \mathbf{E}_3. \quad (21)$$

Here,  $\tilde{\mu}$  represents the angle subtended by  $\tilde{\mathbf{t}}$  with the vector  $\mathbf{E}_1$ . The orientation of the strain gauge in the undeformed state is defined by the vector  $\mathbf{n} \in T_p \Omega_0$  such that  $\mathbf{n}$  makes an angle  $\mu$  with the vector  $\tilde{\mathbf{t}}$ . We have

$$\mathbf{n} = \cos \mu \tilde{\mathbf{t}} + \sin \mu \mathbf{t}. \quad (22)$$

If the cross-section  $\blacksquare_0$  does not vary along the beam in the configuration  $\Omega_0$ , then  $\tilde{\mu} = 0$ . With this construction in hand (as shown in Fig. 2), the scalar or the nominal strain in the strain gauge is obtained as

$$\varepsilon_{\text{discrete}} = \langle \mathbf{F}_3(p) \mathbf{n}, \mathbf{F}_3(p) \mathbf{n} \rangle^{\frac{1}{2}} - 1 \quad (23)$$

## 5 STRESS POWER

Let  $\mathbf{S} = \mathbf{S}_i \otimes \mathbf{E}_i$  represent a two point *first PK stress tensor* such that the internal power for the deformed configuration  $\Omega_j$  is defined as

$$P_{\text{int}}^j = \int_{\Omega_0} \mathbf{S} : \dot{\mathbf{F}}_j d\Omega_0 = \int_{\Omega_0} \mathbf{S} : \dot{\tilde{\mathbf{F}}}_j d\Omega_0 + \int_{\Omega_0} \mathbf{S} : \dot{\mathbf{Q}} \mathbf{Q}^T \mathbf{F}_j d\Omega_0. \quad (24)$$

The anti-symmetric nature of  $\dot{\mathbf{Q}} \mathbf{Q}^T$  can be used to prove that  $\mathbf{S} : \dot{\mathbf{Q}} \mathbf{Q}^T \mathbf{F}_j = 0$  in a fashion similar to Eq. (100) in Chadha and Todd [14]. Therefore, from Eq. (12) and (24), we have,

$$P_{\text{int}}^j = \int_{\Omega_0} \mathbf{S} : \dot{\tilde{\mathbf{F}}}_j d\Omega_0 = \int_{\Omega_0} \sum_{i=1}^3 \langle \mathbf{S}_i, \dot{\tilde{\lambda}}_i^j \rangle d\Omega_0. \quad (25)$$

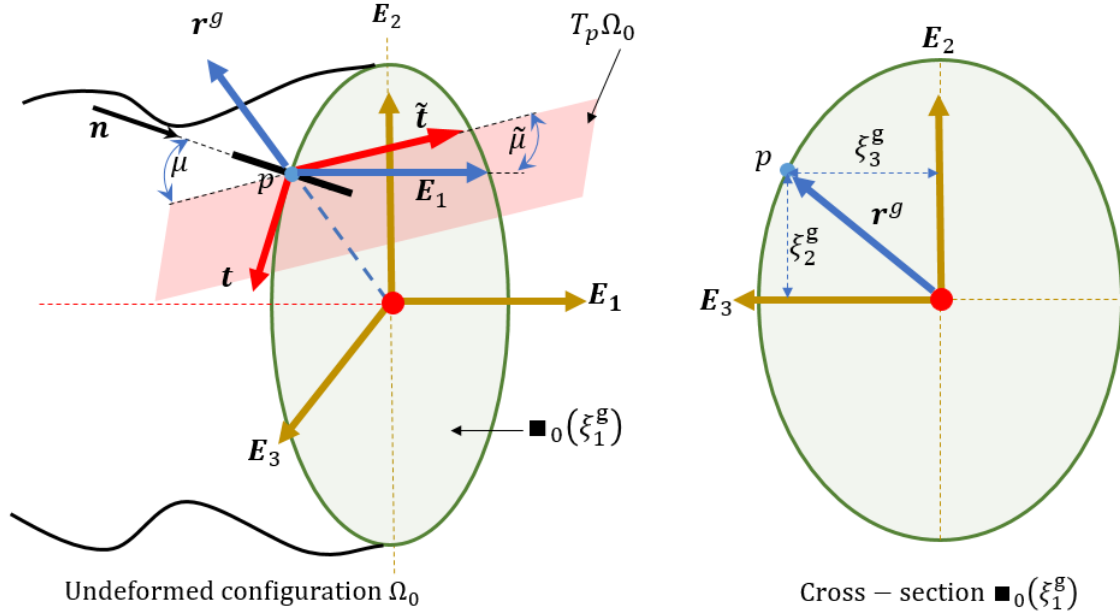


**Figure 2:** Orientation of the discrete strain gauge on the surface of the undeformed configuration.

Recall that the finite strain parameters  $\varepsilon, \kappa, p$  are functions of the arclength  $\xi_1$  only. Therefore, we can simplify (25) in form of a line integral. If we simplify Eq. (25) for  $j = 2$ , the expression of  $P_{\text{int}}^2$  is of same form as Eq. (32) of Simo and Vu-Quoc [7]. Apart from the terms in Eq. (32) of [7], we will have some additional terms in the expression of  $P_{\text{int}}^3$  owing to addition of a fully coupled Poisson's effect.

## 6 CONCLUSION

In this paper, we have presented a comprehensive kinematics of a Cosserat beam considering inhomogeneous material that can capture the effect of multiple curvatures, shear angles, axial strains, coupled Poisson's effect and cross-sectional warping all the while maintaining single manifold character of the problem. We have developed Cosserat structure measurement models for strain gages, which are ubiquitously used for monitoring of such structures in many applications. Finally we obtained the general expression for internal power which is a key parameter to the kinetics of a deformable object.

## REFERENCES

- [1] Duhem, P., 1893, *Le potentiel thermodynamique et la pression hydrostatique*, Annales ecole norm., **10**, pp. 183-230. *Int. J. Num. Meth. Engng.* (1994) **37**:3323–3341.
- [2] Cosserat, E., and Cosserat, F., 1909, *Theorie des Corps Deformable*, Herman, Paris.
- [3] Reissner, E., 1972, "On One-Dimensional Finite-Strain Beam Theory: The Plane Problem," *Journal of Applied Mathematics and Physics* **23**, pp. 795-804.

- [4] Reissner, E., 1973, “*On One-Dimensional Large Displacement Finite Beam Theory,*” *Studies in Applied Mechanics* **52**, pp. 87-95.
- [5] Reissner, E., 1981, “*On Finite Deformation of Space Curved Beams,*” *Journal of Applied Mathematics and Physics* **32**, pp. 734-744.
- [6] Simo, J. C., 1985, “*A finite beam formulation. the three dimensional dynamic problem. part 1,*” *Computer Methods in Applied Mechanics and Engineering*, **49**, pp. 55-70.
- [7] Simo, J. C., Vu-Quoc, L., 1991, “*A Geometrically Exact Rod Model Incorporating Shear and Torsion-Warping Deformation,*” *International Journal of Solids and Structures*, **27**, pp. 371-393.
- [8] Kapania, R. K., Li, J., 2003, “*On geometrically exact curved beam theory under rigid cross-section assumption,*” *Computational Mechanics*, **30**, pp. 428-443.
- [9] Meier, C., 2016, “*Geometrically exact finite element formulations for slender beams and their contact interactions,*” Ph.D Thesis, Technischen Universität, Munich.
- [10] Todd, M. D., Skull, C. J., Dickerson, M., 2013, “*A Local Material Basis Solution Approach to Reconstructing the Three-Dimensional Displacement of Rod-Like Structure from Strain measurements,*” *ASME Journal of Applied Mechanics*, **80** pp. 041028-1 to 041003-10
- [11] Chadha, M., Todd, M. D., 2017, “*A Generalized Approach to Reconstructing the Three-Dimensional Shape of Slender Structures Including the Effects of Curvature, Shear, Torsion, and Elongation,*” *ASME Journal of Applied Mechanics*, **84** pp. 041003-1 to 041003-11
- [12] Chadha, M., Todd, M. D., 2018, “*A Displacement Reconstruction Strategy for Long, Slender Structures from Limited Strain Measurements and Its Application to Underground Pipeline Monitoring,*” In: Conte J., Astroza R., Benzoni G., Feltrin G., Loh K., Moaveni B. (eds) *Experimental Vibration Analysis for Civil Structures. EVACES 2017. Lecture Notes in Civil Engineering*, Springer, Cham, **5** pp. 317-327
- [13] Chadha, M., Todd, M. D., 2018, “*An improved shape reconstruction methodology for long rod like structure using Cosserat kinematics-including the Poisson’s effect,*” In: Kerschen G. (eds) *Nonlinear Dynamics, Volume 1*, conference proceedings of the Society for Experimental Mechanics Series, Chapter 25.
- [14] Chadha, M., Todd, M. D., 2017, “*An introductory treatise on reduced balance laws of Cosserat beams,*” *International Journal of Solids and Structures*, **126-127**, pp. 54-73.